Fermi National Accelerator Laboratory

FERMILAB-Conf-96/221-E

CDF

Quarkonia Production at CDF

A. Sansoni
For the CDF Collaboration

Instituto Nazionale di Fisica Nucleare
00044 Frascati (RM) Italy

Fermi National Accelerator Laboratory
P.O. Box 500, Batavia, Illinois 60510

August 1996

Published Proceedings of the *12th International Conference on Ultra-Relativistic Nucleus-Nucleus Collisions (Quark Matter'96)*, Heidelberg, Germany, May 20-24, 1996.

Operated by Universities Research Association Inc. under Contract No. DE-AC02-76CHO3000 with the United States Department of Energy

Disclaimer

CDF/PUB/BOTTOM/PUBLIC/3804

FERMILAB-CONF-96/221-E

Quarkonia production at CDF

The CDF Collaboration
presented by A. Sansoni[a]

[a]Istituto Nazionale di Fisica Nucleare, 00044 Frascati (RM) Italy. (sansoni@lnf.infn.it)

In the 1992-1995 runs CDF has collected large samples of J/ψ ,$\psi(2S)$ and Υ identified through their muonic decay. In the charmonium system all production sources have been separately measured and compared with the theoretical predictions. A large excess of direct production has been observed for both $\psi(2S)$ and J/ψ . The relative production rate for the χ_c^1 and χ_c^2 has also been measured. The unexpected results have lead to a profound revisitation of the theory of the production of $Q\bar{Q}$ bound states in high energy hadronic collisions.

1. INTRODUCTION

Quarkonium spectroscopy, decay and production have been ideal testing grounds for our ideas on quark dynamics since charmonium was discovered more than twenty years ago. Yet, quarkonium production in hadronic reactions has remained a controversial field. Until recently the color singlet model was believed to give a reasonable description of quarkonium production. In this model it is assumed that a quarkonium state is produced by a free, color singlet, $Q\bar{Q}$ pair with small relative velocity and with the same quantum numbers of the quarkonium state [1]. This short distance process ($O(\alpha_s^3)$ at leading order) is described by perturbative QCD. The formation of the bound state is a long distance, non perturbative, process that can be factored into a parameter either calculable within potential models or extracted from experimental data. This picture has been improved with the inclusion of the next to leading processes where a high p_T parton fragments into a color singlet $Q\bar{Q}$ pair [2]. This is an $O(\alpha_s^4)$ process but, due to the extra p_T^2/m_Q^2 factor, it dominates at the relatively high p_T probed by collider data.

This model predicted that the χ_c has by far the largest cross section [1,3] . Direct production of both J/ψ and $\psi(2S)$ was expected to be small because, due to the extra gluon directly coupled to the $c\bar{c}$ line, these diagrams are suppressed by phase space. The χ_c^0 has a negligible branching ratio into J/ψ therefore prompt J/ψ were expected to originate almost completely from the radiative decays of the χ_c^1 and χ_c^2 . Feed-down is not relevant for the $\psi(2S)$ since it is heavier than the χ_c 's. In collider experiments $c\bar{c}$ states can also arise from the decay of b flavored hadrons. This, non-prompt component was expected to be the dominant source of $\psi(2S)$ and to contribute significantly to J/ψ production.

Prior to the successful operation of the CDF Silicon Vertex Detector, collider data were not too inconsistent with this picture [4]. On the other hand fixed target and ISR collider experiments (where b production is negligible), reported already many years ago that

Pub. Proceedings 12th International Conference on Ultra-Relativistic Nucleus-Nucleus Collisions (Quark Matter 96), Heidelberg, Germany, May 20-24, 1996

χ_c 's were not the primary source of J/ψ [5] in disagreement with the expectations of the color singlet model. More recently CDF has been able to measure the production of J/ψ ,$\psi(2S)$ and χ_c separating the components from b decays and the prompt component. The results were so incompatible with the prediction of the color singlet model that a new theory of quarkonia production has been proposed.

2. DATA SELECTION

The data presented here are from $p\bar{p}$ collisions at $\sqrt{s} = 1.8$ TeV collected with the CDF detector in the 1992-1995 runs. The detector has been described in detail elsewhere [6]. The features most important for these analysis are: 1) the large tracking system contained in the 1.4 T axial magnetic field providing the high resolution momentum measurement of charged particles, 2) the 4-layer Silicon Vertex Detector (SVX) [7] providing the identification of secondary vertices associated with b decays, 3) the Pb-scintillator central electromagnetic calorimeter with a strip chamber embedded at a depth of 5.9 radiation lengths used for the photon reconstruction and 4) the muon chamber system, surrounding the central calorimeter, for the muon identification in the range $|\ \eta\ | < 1.0$.

The J/ψ ,$\psi(2S)$ and Υ 's are reconstructed using their muonic decay. The cutoff associated with the steel of the central calorimeter is $p_T(\mu) > 1.5$ GeV/c. The level 1 trigger efficiency rises from 50% at $p_T(\mu) = 1.6$ GeV/c to 90% at $p_T(\mu) = 3.1$ GeV/c. This implies that only relatively high p_T J/ψ can be reconstructed while, due to its larger mass, Υ 's can be reconstructed down to almost zero p_T . The event selection required:

- Two opposite sign good quality central muons
- $p_T > 2.0$ GeV/c for the soft μ and $p_T > 2.8$ GeV/c for the hard μ
- $p_T^{\mu\mu} > 4.0$ GeV/c and $|\ \eta\ | < 0.6$ for J/ψ and $\psi(2S)$
- $p_T^{\mu\mu} > 0.0$ GeV/c and $|\ y\ | < 0.4$ for Υ 's

The dimuon invariant mass distribution obtained, after this selection, from about $\sim$ 20 pb^{-1} of data is shown in Figure 1.

3. THE $\psi(2S)$ CROSS SECTION

We first review the $\psi(2S)$. In 17.8 pb^{-1} we observe 941 ± 52 $\psi(2S) \rightarrow \mu^+\mu^-$. The measured production cross section is $\sigma \cdot BR(|\ \eta\ | < 0.6,\ p_t > 4.0$ GeV/c$) = (0.849 \pm 0.057(stat) \pm 0.073(sys))$ nb.

The first problem consists in separating between prompt production and feed-down from b decays. With the Silicon Vertex Detector, the prompt and long lived component can be precisely measured. For each $\psi(2S)$ candidate reconstructed in the SVX the two dimensional decay length L_{xy} is calculated. L_{xy} is the projection of the vector $\vec{X}$, pointing from the primary to the secondary vertex, onto the transverse momentum vector of the $\psi(2S)$. The position of the secondary vertex is obtained by constraining the two muons to come from a common decay point. To convert L_{xy} into a proper lifetime we use $(\beta\gamma)$

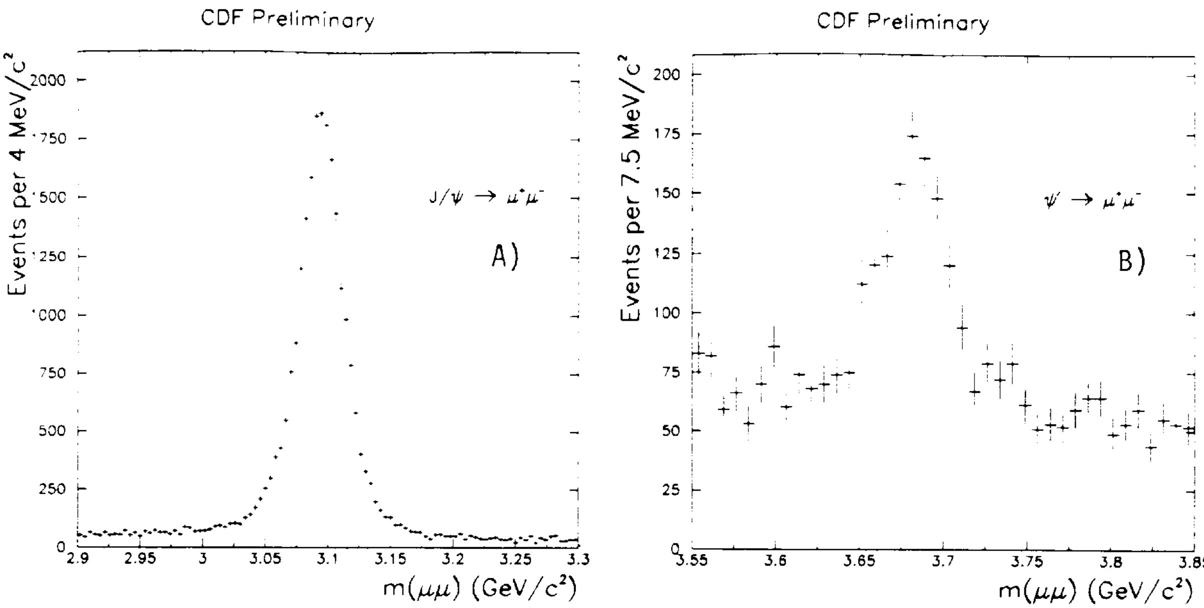

Figure 1. Dimuon invariant mass distribution. A) In the J/ψ signal region; B) in the $\psi(2S)$ signal region.

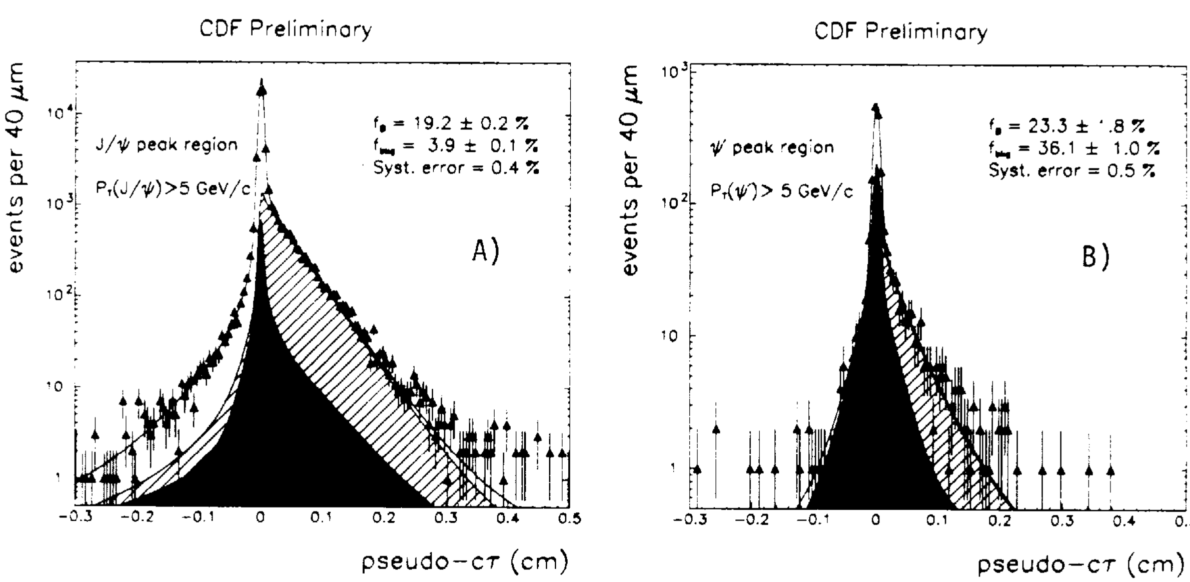

Figure 2. $c\tau_{pseudo}$ distribution decomposed into prompt (unshaded), from B's (hatched), and background (dark shading). A) For the J/ψ candidates; B) for the $\psi(2S)$ candidates.

of the $\psi(2S)$ and a correction factor F_{corr}, determined from Monte Carlo, to take into account the difference with $(\beta\gamma)$ of the b hadron.

$$c\tau_{pseudo} = \frac{L_{xy}}{(P_t^{\psi}/M^{\psi}) \cdot F_{corr}} \quad , \qquad\qquad L_{xy} = \vec{X} \cdot \vec{P_t^{\psi}} / P_t^{\psi} \qquad (1)$$

Figure 2 shows the resulting $c\tau_{pseudo}$ distribution.

To determine the fraction from b's we fit this distribution with the sum of three contributions: 1) the prompt component parametrized with a gaussian, 2) the long lived component parametrized with an exponential smeared with the detector resolution (hatched in Figure 2) the background component obtained from the sidebands of the $\psi(2S)$ (dark shading in Figure 2). The result is that $23.3 \pm 1.8\%$ of the $\psi(2S)$ come from b decays, by far the majority is unambiguously prompt.

There is sufficient data do this fit in several p_T bins, the fraction of $\psi(2S)$ from b's slowly increase with p_T . From this measurement we derive the differential cross section for $\psi(2S)$ from b's and for prompt $\psi(2S)$. This is shown in Figure 3 together with the theory curves. The b component is in reasonable agreement with the NLO QCD theory prediction while the prompt component is about a factor of 50 over the color singlet theoretical curve [3], the other curves shown in this figure will be described in section 5.

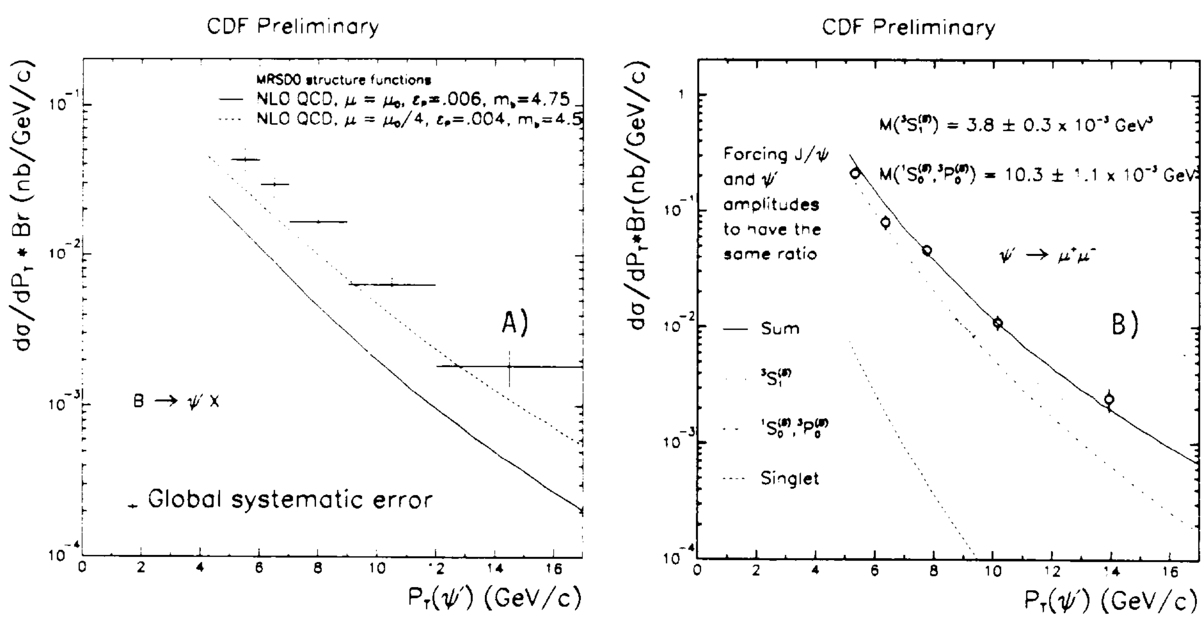

Figure 3. $\psi(2S)$ differential cross section. A) $\psi(2S)$ from B's, the curves are NLO QCD calculations; B) Prompt $\psi(2S)$, the curves show the color singlet component, the two color octet components and their sum.

This large discrepancy was nicknamed the "CDF $\psi(2S)$ anomaly" and ignited the renewed interest in quarkonia production. Two proposals were put forward to explain the disagreement. The first one was that charmonium states above the $D\bar{D}$ threshold, whose decay in open charm is forbidden, or new exotic states, decay in $\psi(2S)X$ accounting for the excess [8]. The other proposal was that the basic assumption of the color single model need not be true and $c\bar{c}$ pairs produced at short distance in a color octet state must be an important additional source of $\psi(2S)$ [9].

To better understand the origin of this discrepancy it is natural, from the experimental point of view, to see if this excess is a feature of the $\psi(2S)$ only or it is also found in J/ψ production.

4. THE J/ψ CROSS SECTION

For the J/ψ the number of events used is $26,545 \pm 177$ and the integrated production cross section is $\sigma \cdot BR(|\eta| < 0.6,\ p_t > 4.0$ GeV/c$) = (32.71 \pm 0.29(stat) \pm 2.9(sys))$ nb. The prompt and b component are measured fitting the $c\tau_{pseudo}$ distribution in the same way described for the $\psi(2S)$. The corresponding distribution is also shown in Figure 2. The fraction of J/ψ from b's is $19.2 \pm 0.2\%$, similar to the $\psi(2S)$, and the cross section of J/ψ from b's is also in decent agreement with theory.

The prompt J/ψ cross section is again underestimated by the theoretical prediction, although only by a factor of ~ 6. But in this case the the prompt component includes both direct J/ψ production and feed-down from χ_c . It is therefore important to compare data and theory for the direct J/ψ and χ_c components separately. This can be done reconstructing the $\chi_c \rightarrow J/\psi\,\gamma$ decay and measuring the fraction of J/ψ that originates from this source (decay modes of the χ_c including a J/ψ , other than the $\chi_c \rightarrow J/\psi\,\gamma$, are expected to be small [10]).

The χ_c analysis is based on $32,642 \pm 181$ J/ψ candidates reconstructed in about 20 pb^{-1} of data. To reconstruct the $\chi_c \rightarrow J/\psi\,\gamma$ we combine the J/ψ with photon candidates found in the event. A photon candidate is defined by a central electromagnetic calorimeter tower with energy $E^\gamma > 1.0$ GeV associated with a strip chamber cluster and no tracks pointing to the tower. The cluster position and the interaction vertex define the photon direction, this together with the calorimeter energy measurement determines the photon momentum. The mass difference, ΔM, between the dimuon-photon mass and the dimuon mass is shown in Figure 4, a peak of $1,230 \pm 71$ events is observed at the mass of about 400 MeV/c^2 corresponding to the χ_c states. The width of the signal is about 60 MeV/c^2, too large to distinguish the χ_c^1 and χ_c^2 separated by 45.7 MeV/c^2. The data allow to observe significative signals in four J/ψ p_T bins.

We obtain the shape of the background with a Monte Carlo method that uses the real J/ψ events as input. Each charged track in the event is assumed to be a π^0 , η or K_s in ratios predicted by the measured K/π and η/π^0 ratios and isospin symmetry. The particles are decayed and the resulting photons simulated through the detector. Applying the χ_c reconstruction to this event gives a ΔM distribution that is our model for the shape of the background. The number of signal events is extracted fitting the data to the sum of a gaussian and this background shape. To test this model we compared the ΔM distribution obtained in this way with the one directly obtained from the data, both for dimuon pairs in the sidebands of the J/ψ peak where there is no χ_c signal, and the agreement is very good as shown in the inset of Figure 4.

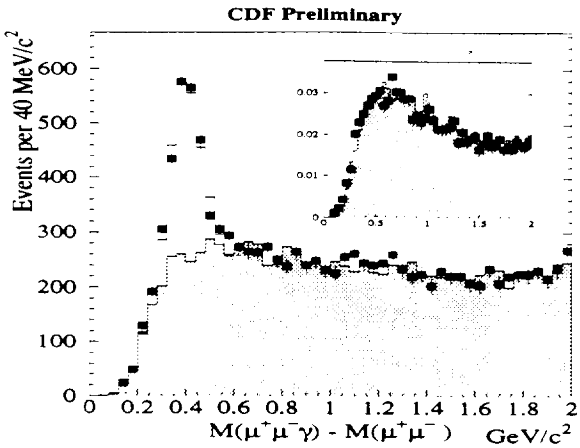

Figure 4. Mass difference $M(\mu^+\mu^-\gamma) - M(\mu^+\mu^-)$ for the ψ signal region in 40 MeV/c^2 bins. The points show the data histogram, the shaded histogram is the background shape predicted by our background Monte Carlo. The solid line is the fit to the data of a gaussian signal plus the background histogram. The inset shows the comparison in the ψ sidebands.

The photon reconstruction efficiency is obtained using conversion electrons found in the data and correcting for the known differences in detector response between photons and electrons. After correcting for the photon acceptance and reconstruction efficiency we obtain a fraction of J/ψ from χ_c of $(28.8 \pm 1.7(stat) \pm 6.4(sys))\%$.

This fraction includes a contribution from $B \rightarrow J/\psi\ X$ and $B \rightarrow \chi_c\ X$ that must be removed. We do this using the same technique used for the J/ψ and $\psi(2S)$ applied to the reconstructed χ_c . This correction is small, the fraction of J/ψ from χ_c without the contribution from b's is $(31.2 \pm 1.8(stat) \pm 7.1(sys))\%$ and is shown as function of the J/ψ p_T in Figure 5. Figure 6 shows the cross section for J/ψ from χ_c and for direct J/ψ , both with the b contribution removed. The normalization of the J/ψ from χ_c cross section is in agreement with the theoretical calculation while the direct J/ψ data is again a factor ~ 50 over the prediction.

We conclude that the color singlet model of charmonium production fails to describe direct production, both for the $\psi(2S)$ and the J/ψ by about the same large amount. Contrary to its prediction direct production is the dominant source of prompt $\psi(2S)$ and J/ψ . This data does not exclude the possibility of a contribution from $c\bar{c}$ states above the open charm threshold, but makes this an unlikely explanation for the large excess of direct $\psi(2S)$ and J/ψ .

5. THE COLOR OCTET MECHANISM

Having found the same excess of direct $\psi(2S)$ and J/ψ it is natural to question the basic assumption of the color singlet model. In fact even in the color singlet model a color octet

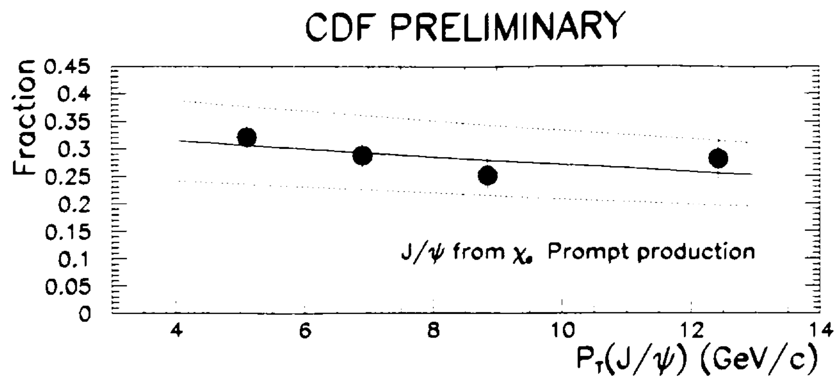

Figure 5. Fraction of J/ψ from χ_c as function of the J/ψ p_T with the contribution from b's removed.

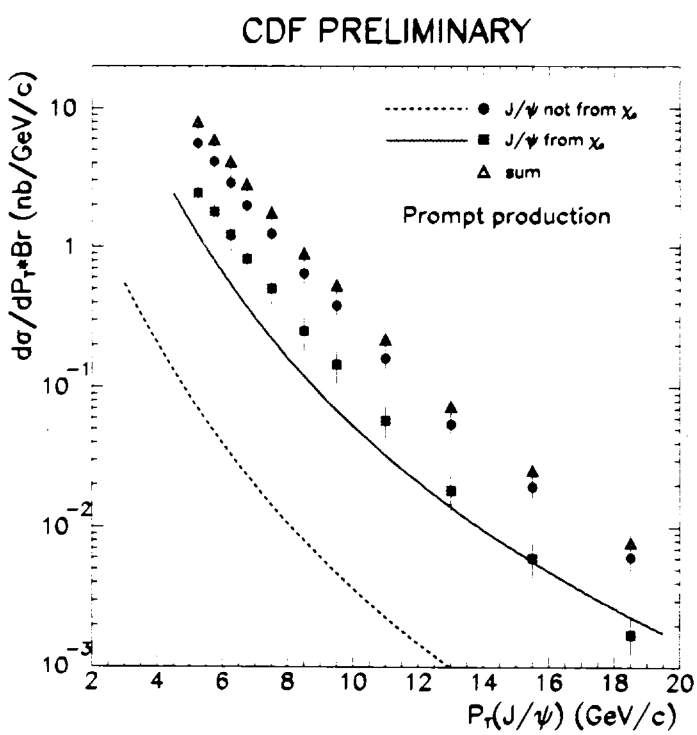

Figure 6. J/ψ differential cross sections as a function of J/ψ p_T with the contribution from b's removed; the circles show the direct component, the squares correspond to J/ψ from χ_c and the triangle is the sum. The curves are the color singlet NLO QCD calculations.

contribution is required to cancel infrared divergences in the calculation of the P-wave states cross section. The diagrams responsible for the production of the S-wave states are not divergent and a color octet contribution is not required for perturbative consistency but it is natural to attempt an explanation of the excess of S-wave production in terms of the missing color octet contribution. In this mechanism the $c\bar{c}$ pair is produced, at short distance, in a color octet state with a spectrum of quantum numbers and evolves, non-perturbatively, into a color singlet bound state radiating soft gluons. This idea is reminiscent of the old color evaporation model but has been developed in a new rigorous formalism describing quarkonia annihilation and production [11]. The predictive power of this theory is not as strong as for the color singlet model because the normalization of the non-perturbative matrix elements cannot be computed and must be extracted fitting the experimental data. However, the theory has distinctive predictive power: the p_T dependence can be calculated and direct J/ψ and $\psi(2S)$ production at large p_T is predicted to be transversely polarized. Ultimately, since there are amplitudes that contribute to different processes, the matrix elements derived from a fit to a given reaction can be used to predict a different process. This involves comparing quarkonia production data from e^+e^-, ep, $p\bar{p}$ colliders, fixed target pN, πN and, last but not least, heavy nuclei collisions. An excellent and complete review of these theoretical developments can be found in reference [12] and in these proceedings [13].

In direct J/ψ and $\psi(2S)$ production three amplitudes are expected to dominate corresponding to color octet $c\bar{c}$ pair in the states ${}^3S_1$, ${}^3P_J$ and ${}^1S_0$. The first term dominates at high p_T , the second and third term dominate at low p_T and have similar shape in p_T . Based on a recent calculation [14] of these contributions we have performed a fit to our direct J/ψ and $\psi(2S)$ cross section to determine the matrix elements, $\mathrm{M}({}^3S_1^{(8)})$ and $\mathrm{M}({}^1S_0^{(8)},{}^3P_J^{(8)})$, where we have summed the second and third term because they cannot be distinguished in our data. Since the matrix elements should be similar for the J/ψ and $\psi(2S)$ and the ratio $\mathrm{M}({}^3S_1^{(8)})/\mathrm{M}({}^1S_0^{(8)},{}^3P_J^{(8)})$ should be of the order of the charm quark velocity v_c in the bound state we have performed a simultaneous fit to the direct J/ψ and $\psi(2S)$ cross section with the requirement that the ratio of the two amplitudes be the same. The contribution of $\psi(2S) \rightarrow J/\psi\ \pi\ \pi$ to the J/ψ was also taken into account in the combined fit. The result of this fit is shown in Figures 3 and 7, Figure 8 shows the ratio of direct cross section. The amplitudes determined by the fit are $\mathrm{M}({}^3S_1^{(8)}) = (3.8 \pm 0.3) \times 10^{-3}$ GeV^3, $\mathrm{M}({}^1S_0^{(8)},{}^3P_J^{(8)}) = (10.3 \pm 1.1) \times 10^{-3}$ GeV^3 for the $\psi(2S)$ and $\mathrm{M}({}^3S_1^{(8)}) = (11.0 \pm 0.8) \times 10^{-3}$ GeV^3, $\mathrm{M}({}^1S_0^{(8)},{}^3P_J^{(8)}) = (29.9 \pm 3.1) \times 10^{-3}$ GeV^3 for the J/ψ . These matrix elements differ by about a factor of three between the $\psi(2S)$ and J/ψ and the ratio is of the order of the expected charm quark velocity $v_c \sim 1/3$. While our data can be described reasonably well by the inclusion of the color octet contribution a conclusion on the validity of this model can be drawn only after comparing with other processes sensitive to the matrix elements determined in this fit.

Another test of the theory will be provided by polarization measurements. States produced by color octet gluons inherit the spin alignment of the nearly on-shell gluons therefore directly produced J/ψ and $\psi(2S)$ should be strongly transversely polarized. In fixed target experiments the J/ψ polarization is known to be consistent with zero and this fact has been considered as an indication that the color octet mechanism cannot provide a

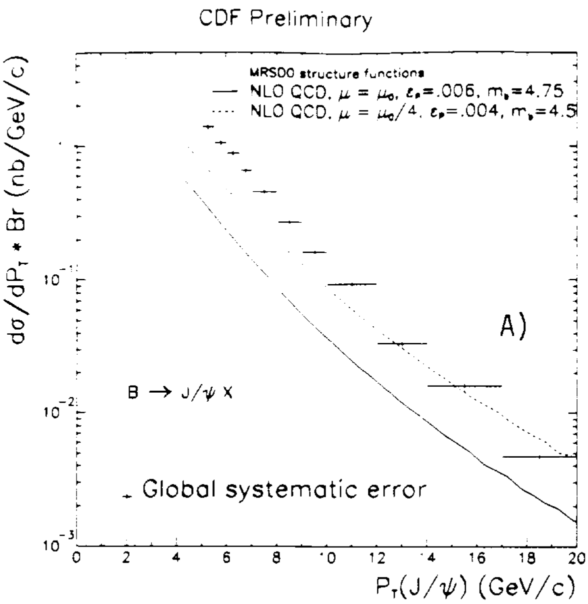

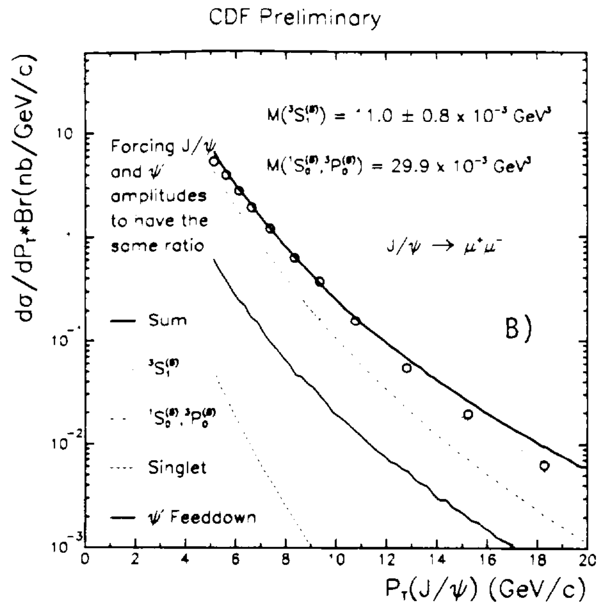

Figure 7. J/ψ differential cross section. A) J/ψ from B's, the curves are NLO QCD calculations; B) Prompt J/ψ not from χ_c , the curves show the color singlet component, the contribution from the $\psi(2S)$, the two color octet components and their sum.

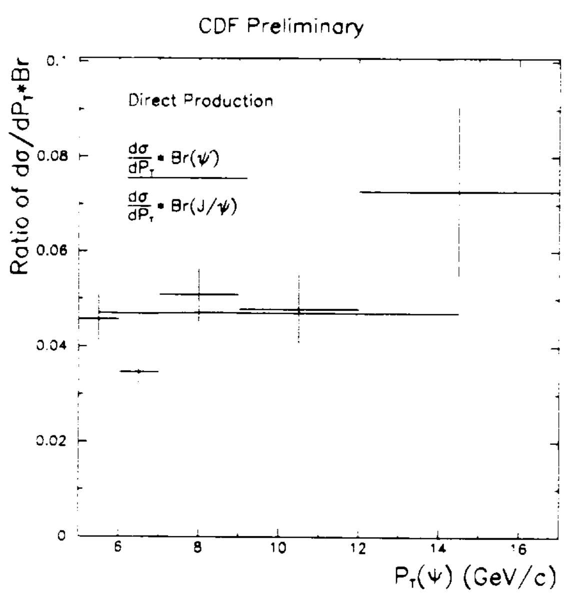

Figure 8. Ratio between $\psi(2S)$ and J/ψ direct cross section.

satisfactory explanation of charmonia production [15]. The predictions are more reliable in the high p_T region probed by collider data therefore the polarization measurement currently in progress at CDF is likely to provide the crucial test.

6. THE χ_c^1 AND χ_c^2 RECONSTRUCTION

As noted earlier this analysis has insufficient resolution to distinguish the two χ_c states. A complementary analysis can be done requiring that the photon has converted into an e^+e^- pair. With this method the photon reconstruction uses only tracking information greatly improving the χ_c mass resolution. The efficiency of this reconstruction is low, therefore this analysis utilizes a larger data sample corresponding to 110 pb^{-1}. Events are selected requiring the photon to have $p_T > 1.0$ GeV/c and a conversion vertex separated from the primary interaction vertex by more than 1.0cm in the transverse plane. To select prompt χ_c candidates we use only J/ψ reconstructed in the SVX and require $c\tau_{pseudo} < 100\mu$m. The resulting $J/\psi\gamma$ mass distribution is shown in Figure 9. The χ_c^1 and χ_c^2 peaks are nicely separated. The number of events in the peaks, with a small acceptance correction and the known decay branching ratios, are used to obtain the relative production cross section of:

$$\frac{\sigma(\chi_c^2)}{\sigma(\chi_c^1)+\sigma(\chi_c^2)} = 0.47 \pm 0.08(stat) \pm 0.02(sys)$$

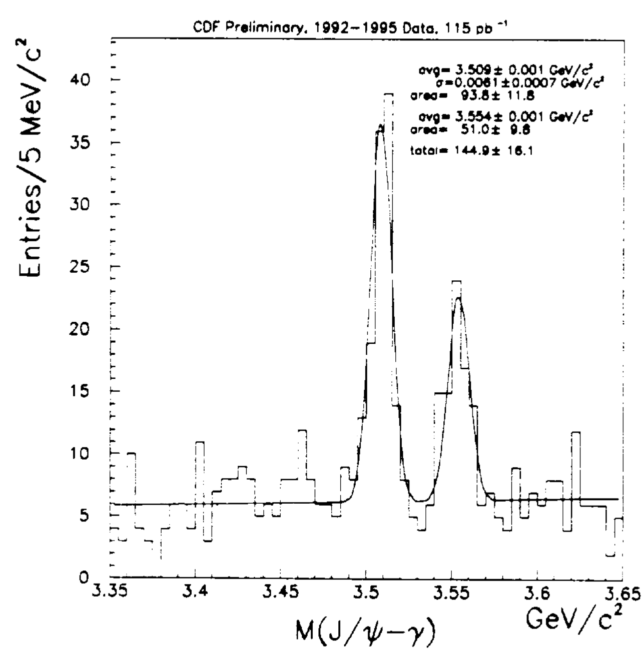

Figure 9. The $J/\psi\gamma$ mass distribution, based on tracking measurement via photon conversion, for prompt J/ψ .

7. THE Υ CROSS SECTION

In the $b\bar{b}$ system CDF has measured the differential cross section for the Υ 's [16]. In 17 pb^{-1} of data we have reconstructed $\sim$ 1200 $\Upsilon(1S)$, $\sim$ 300 $\Upsilon(2S)$ and $\sim$ 200 $\Upsilon(3S)$, Figure 10 shows the dimuon invariant mass distribution in the Υ region after the selection described in section 2.

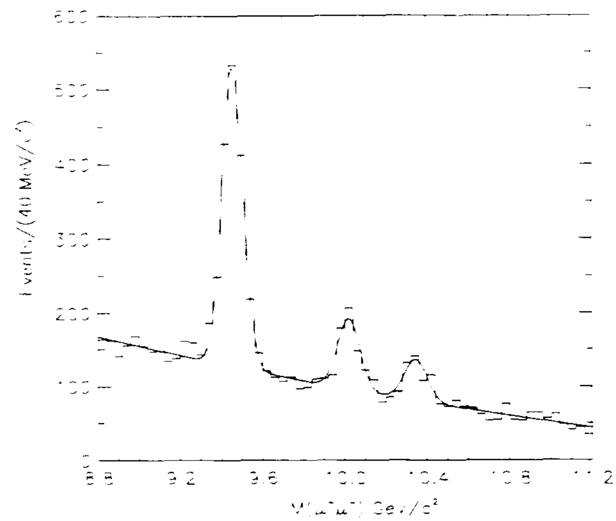

Figure 10. Dimuon invariant mass distribution in the Υ region.

The production cross sections measured in the rapidity range $\mid y \mid < 0.4$ are:

$$\sigma \cdot BR(\Upsilon(1S)) = (753 \pm 29(stat) \pm 72(sys))\ \text{pb},\ p_t > 0\ \text{GeV/c}$$
$$\sigma \cdot BR(\Upsilon(2S)) = (183 \pm 18(stat) \pm 24(sys))\ \text{pb},\ p_t > 1\ \text{GeV/c}$$
$$\sigma \cdot BR(\Upsilon(3S)) = (101 \pm 15(stat) \pm 13(sys))\ \text{pb},\ p_t > 1\ \text{GeV/c}$$

The differential cross sections are shown in Figure 11. The theoretical curve is a leading order QCD calculation that includes the contributions from all the known χ_b states and feed-down from the S states. The measured cross sections are higher than the calculations by a factor $\sim$ 3 for the $1S$ and $2S$ and $\sim$ 10 for the $3S$. Including the contribution from the decay of the yet unobserved $\chi_b(3P)$ the larger disagreement for the $\Upsilon(3S)$ is reduced.

For the Υ 's the experimental analysis, at this time, is not as complete as it is in the charmonium system because the contribution from the χ_b's has not been separated. The $\chi_b \rightarrow \Upsilon\gamma$ reconstruction is extremely difficult at CDF because we are sensitive to low p_T χ_b and the resulting photon will be too soft to be detected with reasonable efficiency.

Therefore firm conclusion on whether there is an excess of direct production or not can not be definitively drawn. For the Υ 's the shape of the differential cross section is also not reproduced by the calculation in the low p_T region, but it has been shown that including a parton k_T smearing agreement in the shape can be obtained.

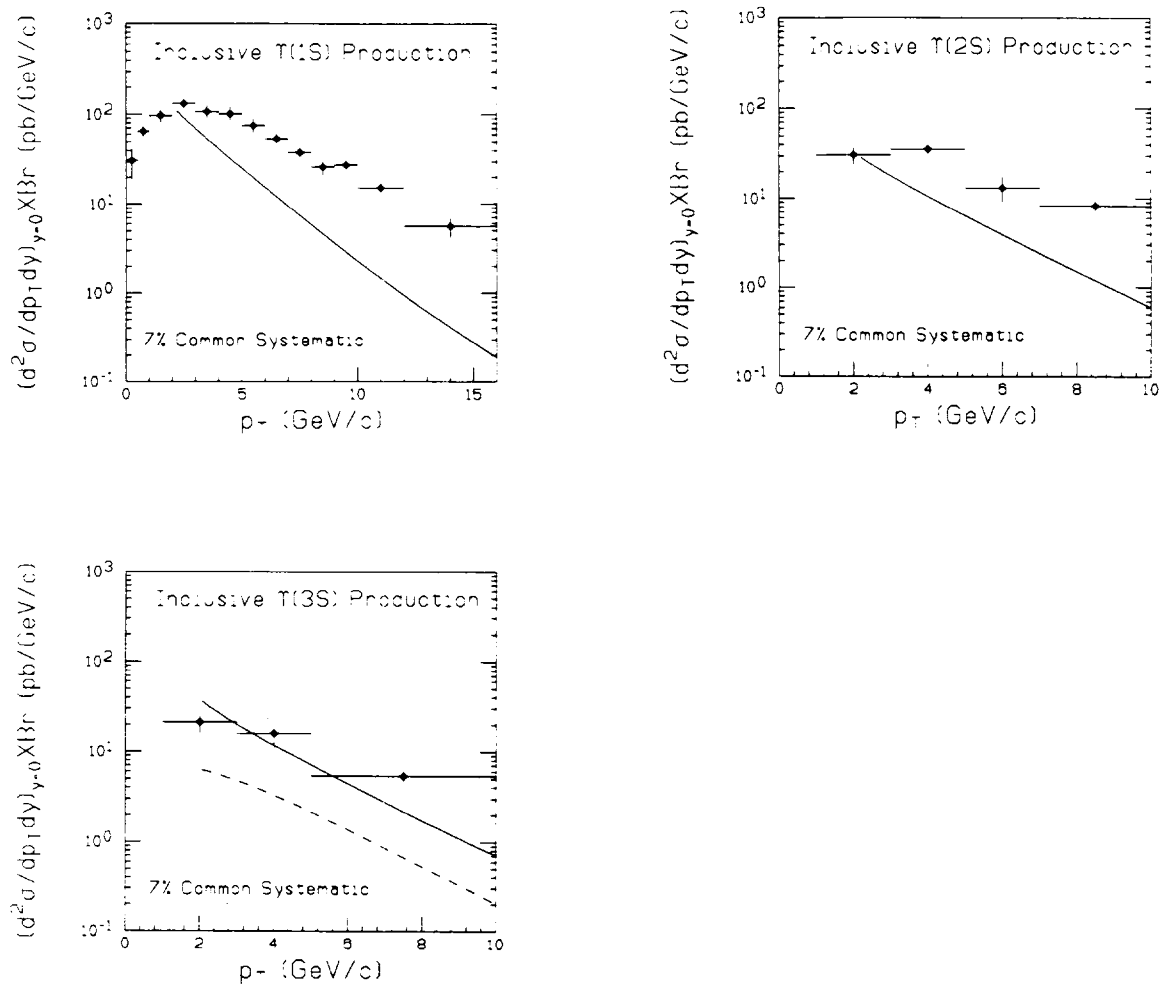

Figure 11. Υ differential cross sections as a function of p_T The curves are the LO QCD calculations.

8. CONCLUSIONS

CDF data on J/ψ ,$\psi(2S)$,χ_c and Υ production has unraveled surprises. The color singlet model based on perturbative QCD, previously believed to give a reasonable description of quarkonia production, dramatically fails to reproduce the data. By disentangling all production sources (from b's and direct, for the $\psi(2S)$; from b's from χ_c 's and direct, for the J/ψ) CDF found that direct production is the main production mechanism of prompt J/ψ and $\psi(2S)$ in disagreement with the expectations by a factor of 50. Charmonium production in fixed target experiments is reviewed elsewhere in these proceedings [17] and shows a remarkably similar pattern. A new description of quarkonia production, including the color octet mechanism, has been proposed and the CDF data have been used to extract the normalization of the color octet matrix elements. These amplitudes can be used to predict charmonium production in other reactions thus allowing a test of the new model. CDF data will soon provide another test by measuring the polarization of the directly produced $\psi(2S)$.

REFERENCES

1. R. Baier and R. Ruckl, Z.Phys. C19 (1983) 251
   E.W.N. Glover, A.D. Martin, W.J. Stirling, Z.Phys. C38 (1988) 473.
2. E.Braaten and T.C. Yuan, Phys.Rev.Lett. 71 (1993) 1673.
3. E. Braaten, *et al.*, Phys.Lett. B333 (1994) 548;
   M.Cacciari, M.Greco, Phys. Rev. Lett. 73 (1994) 1586.
4. UA1 Coll.,C. Albajar *et al.*, Phys.Lett. B256 (1991) 112;
   CDF Coll.,F. Abe *et al.*, Phys.Rev.Lett. 69 (1992) 3704;
   CDF Coll.,F. Abe *et al.*, Phys.Rev.Lett. 71 (1993) 2537.
5. C. Korkoumelis *et al.*, Phys.Lett. B81 (1979) 405;
   Y. Lemoigne *et al.*, Phys.Lett. B113 (1982) 509;
   S.R. Hahn *et al.*, Phys. Rev. D30 (1984) 671;
   D.A. Bauer *et al.*, Phys.Rev.Lett. 54 (1985) 753.
6. F. Abe *et al.*, Nucl. Instrum. Methods A271 (1988) 387.
7. D. Amedei *et al.*, Nucl. Instrum. Methods A350 (1994) 73.
8. F.E.Close, Phys.Lett. B342 (1995) 369;
   D.P.Roy and Sridhar, Phys.Lett. B345 (1995) 537;
   P.Cho M.Wise and Trivedi, Phys.Rev. D51 (1995) 2039.
9. E.Braaten and S.Fleming, Phys.Rev.Lett. 74 (1995) 3327;
   P.Cho and M.Wise, Phys.Lett. B346 (1995) 129;
   M.Cacciari,M.Greco,M.L.Mangano,A.Petrelli,Phys.Lett. B356 (1995) 553.
10. E.L.Barger and C.Sorensen, Phys.Rev. D24 (1981) 2019.
11. G.T. Bodwin, E.Braaten and G.P.Lepage, Phys.Rev. D51 (1995) 1125.
12. E. Braaten, OHSTPY-HEP-T-96-001,MADPH-96-927,UCD-96-2,hep-ph/9602374.
13. E. Braaten, these proceedings
14. P.Cho and A.K. Leibovich, Phys.Rev. D53 (1996) 150;
    P.Cho and A.K. Leibovich, Phys.Rev. D53 (1996) 6203.
15. S.J. Brodsky *et al.* Phys.Rev. D51 (1995) 3332;
    Wai-Keung Tang and M.Vattinen, Phys.Rev. D53 (1996) 4851;
    Wai-Keung Tang and M.Vattinen, NORDITA-96/18-P,hep-ph/9603266
16. CDF Coll.,F. Abe *et al.*, Phys.Rev.Lett. 75 (1995) 4358.
17. P.L. McGaughey, these proceedings